Decomposition and stoichiometry variation in lithium hydride and lithium deuteride

Stratton, Brandon; Davis, Thomas; Astbury, Jack; Abdallah, Mohammad; Stephens, Simon; Middleburgh, Simon

Journal of Nuclear Materials

E-pub ahead of print: 01/02/2025

Publisher's PDF, also known as Version of record

Journal of Nuclear Materials 606 (2025) 155619

Contents lists available at ScienceDirect

Journal of Nuclear Materials

journal homepage: www.elsevier.com/locate/jnucmat

Decomposition and stoichiometry variation in lithium hydride and lithium deuteride

Brandon J. Stratton [a], Thomas P. Davis [a], Jack O. Astbury [b], Mohamad Abdallah [b], Simon Stephens [a], Simon C. Middleburgh [a,*]

[a] Nuclear Futures Institute, Bangor University, Dean Street, Bangor, Gwynedd, LL57 1UT, United Kingdom
[b] Tokamak Energy Ltd, 173 Brook Drive, Milton Park, Oxfordshire, OX14 4SD, United Kingdom

ARTICLE INFO

Keywords:
Lithium
Breeder material
Hydrides
Decomposition
DFT

ABSTRACT

The decomposition of the lithium hydride isotopologues (^{6}LiH, ^{6}LiD, ^{7}LiH and ^{7}LiD) and their propensity to accommodate non-stoichiometry is predicted using atomistic modelling methods. Significant differences exist between the reaction enthalpies of the isotopologues with respect to the hydrogen isotope, whilst negligible differences exist with respect to the incorporated lithium isotope. The calculated defect concentration identifies the vacancy formation energy for LiH is significantly lower than for LiD at a defined temperature. Further, the temperatures of complete decomposition to lithium metal for LiH and LiD are reported as 959 K and 999 K, respectively, a 40 K difference of potential use in breeder blanket concepts. The predicted decomposition of LiH is in good agreement with the experimentally observed value of 962 K. Defect concentrations at the decomposition temperature for all isotopologues are similar, despite the changes in temperature.

1. Introduction

In the relentless pursuit of sustainable energy solutions, the realm of energy storage materials and fusion materials play a pivotal role in shaping the future of low carbon energy technologies. Among these materials, lithium hydride (LiH) has emerged as a promising candidate material for a number of applications. This research article represents the first assessment of the decomposition behaviour of LiH using atomic scale modelling techniques to provide a mechanistic assessment of the system and the impact of isotope variation within the structure.

Lithium hydride is a binary compound comprising lithium and hydrogen, in the rock-salt structure (space group 225: $Fm\bar{3}m$) [1]. It has a high melting/decomposition temperature compared to many other hydrides, suggesting its potential use in a range of engineered components [2]. Outside of the nuclear industry, uses of lithium hydride include: the production of reagents for organic synthesis (such as $Li[BH_4]$), high density and compact solid hydrogen storage, and as a fuel for hydrogen internal combustion engines [3–5].

The Li-LiH phase diagram has been reported and discussed previously [6]. Reported here in Fig. 1, a small region of the phase diagram is solid β-phase (LiH), indicating small deviations from stoichiometry are expected, increasing with temperature. Across other non-stoichiometric mole fractions, a broad mixed phase exists ($\alpha_l + \beta_s$) across most temperatures below the lithium hydride melting point.

The influence of the hydrogen isotope present in a variety of materials on properties and thermodynamics has been assessed previously, and an example of this is the experimental research undertaken by R. Liu et al. [7] who used experimental techniques to show that a differing Pd-Pt structure resulted in a modified rate of dissolution of hydrogen, and also reported a significant difference in the activation energy required for hydrogen/deuterium absorption and dissolution relative to the hydrogen isotope present within the alloy.

Further experimental work by Akimovich et al., specifically analysing LiH and LiD, identified the differing behaviour of the two hydrogen isotopes with temperature, focusing on the Li rich region [6]. Akimovich et al. report an experimental assessment highlighting the difference in solidification temperature, and isotopic dependence of the melting point of the Li-Li(H/D) monotectics.

Olsson et al. [8] studied the effects of variable stoichiometries on zirconium hydrides and zirconium deuterides with variable stoichiometries, using *ab initio* methods over a range of temperatures, determining the thermodynamic properties of each of the materials. Notably, they calculated qualitative differences between the zirconium hydrides and deuterides across most of the analysed properties including entropy,

* Corresponding author.
E-mail address: s.middleburgh@bangor.ac.uk (S.C. Middleburgh).

https://doi.org/10.1016/j.jnucmat.2025.155619
Received 15 October 2024; Received in revised form 6 January 2025; Accepted 7 January 2025

Available online 15 January 2025

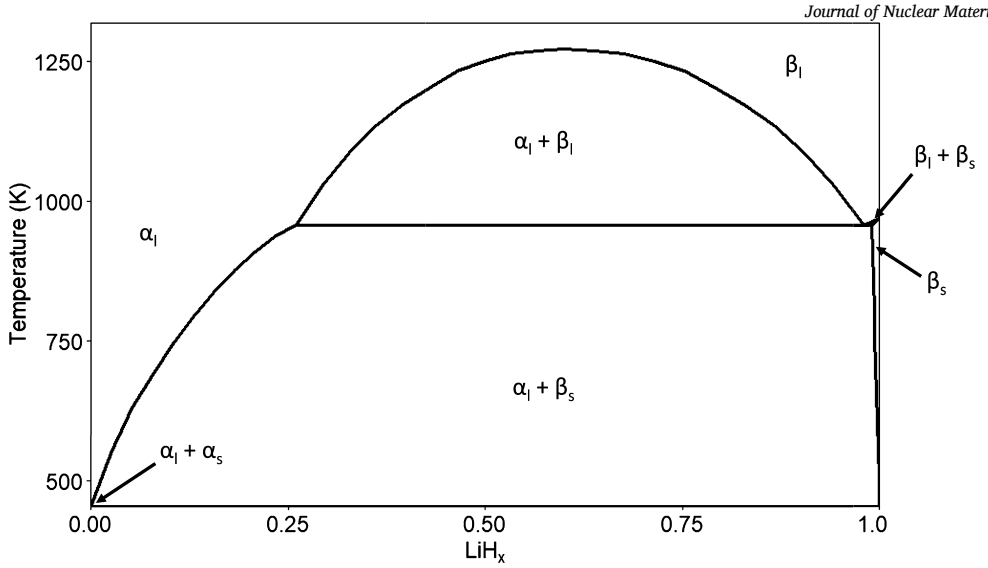

Fig. 1. Li-LiH phase diagram. This phase diagram shows the mole fraction (x) of lithium hydride and lithium against temperature as presented by KA Yakimovich et al. [6].

heat capacity and Debye temperature; It was determined that ZrH_x and ZrD_x have a difference in formation enthalpy for each of the compositions, with the deuterium containing compositions having a larger formation energy than the hydrogen containing compositions, both of which aligned with previous experimental results.

Notably, similar research investigating the non-stoichiometric effects of lithium within lithium hydride has been assessed using first-principle methodologies, focusing on the impact of the modified stoichiometry on the hydrogen storage capacity [9]. This study, alongside similar investigations into the modification of the metallic components of the crystal structure [10], highlighted that both the elemental composition and the stoichiometry of the material have an observable impact on the decomposition temperature and overall structure of the materials analysed, further motivating additional exploration of this topic towards an isotopically modified composition of lithium hydride.

This research aims to explore the impact of both the hydrogen isotope and the lithium isotope present within the composition and how they impact the material's decomposition temperature and deviation in stoichiometry.

2. Methodology

Density functional theory was used to investigate the differences between the isotopologues' thermodynamic behaviour. The calculations were performed using the Vienna Ab initio Simulation Package (VASP) [11] version 6.3.0, where the inter-atomic force constants were calculated using the projector augmented wave (PAW) method, [12] with the generalised gradient approximation (GGA) of Perdew, Burke and Ernzerhof (PBE) exchange-correlation functional [13].

After sensitivity studies, calculations using 2 × 2 × 2 supercells of LiH (containing 64 lattice sites, shown in Fig. 2) were performed with a 5 × 5 × 5 k-point mesh and a plane wave energy cut-off of 650 eV (k-point mesh was scaled appropriately for supercells of a different size). These were used to provide the input structures and data for phonon informed preductions using the Phonopy sotfware, described shortly. The atomic force threshold energy for geometry optimisation was set to 10^{-7} eV/Å and the electronic relaxation threshold defined as 10^{-8} eV. This was essential to provide the accuracy greater than 10^{-7} eV in the system's total energy, required to maximise the accuracy of post-process calculations, as determined through convergence testing.

Compounds containing elements which have multiple isotopes can have a variety of isotopic combinations, known as isotopologues.

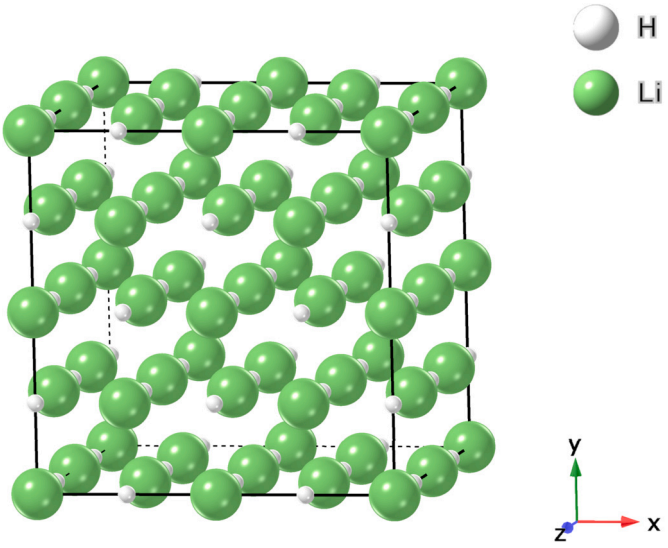

Fig. 2. A 2×2×2 supercell of lithium hydride. This is the crystalline structure of lithium hydride with lithium represented by green spheres and hydrogen represented by white spheres. (For interpretation of the colours in the figure(s), the reader is referred to the web version of this article.)

Lithium hydride has four stable (non-radioactive) isotopologues consisting of combinations of ^{6}Li, ^{7}Li, ^{1}H (protium, H) and ^{2}H (deuterium, D). This research will assess all four of these lithium hydride isotopologues: ^{6}LiH, ^{6}LiD, ^{7}LiH and ^{7}LiD.

Supercells with a single hydrogen vacancy intrinsic defect ($V_H^{/}$), were used for the simulation of partial dehydriding (equation (1)) [14,15], whilst the complete dehydriding is considered through equation (2) with body-centered cubic lithium metal being formed. For the lithium metal structure, a 2 × 2 × 2 cubic supercell consisting of 16 atoms was used with a k-point mesh of 7 × 7 × 7.

$$H_H \longrightarrow V_H + \frac{1}{2}H_{2(g)} \quad (1)$$

$$LiH_{(s)} \longrightarrow Li_{(s)} + \frac{1}{2}H_{2(g)} \quad (2)$$

During the initial relaxation of the requisite structures, the atomic positions, size and shape of the supercells were unrestrained, allowing relaxation to their optimised geometries. The Phonopy software package

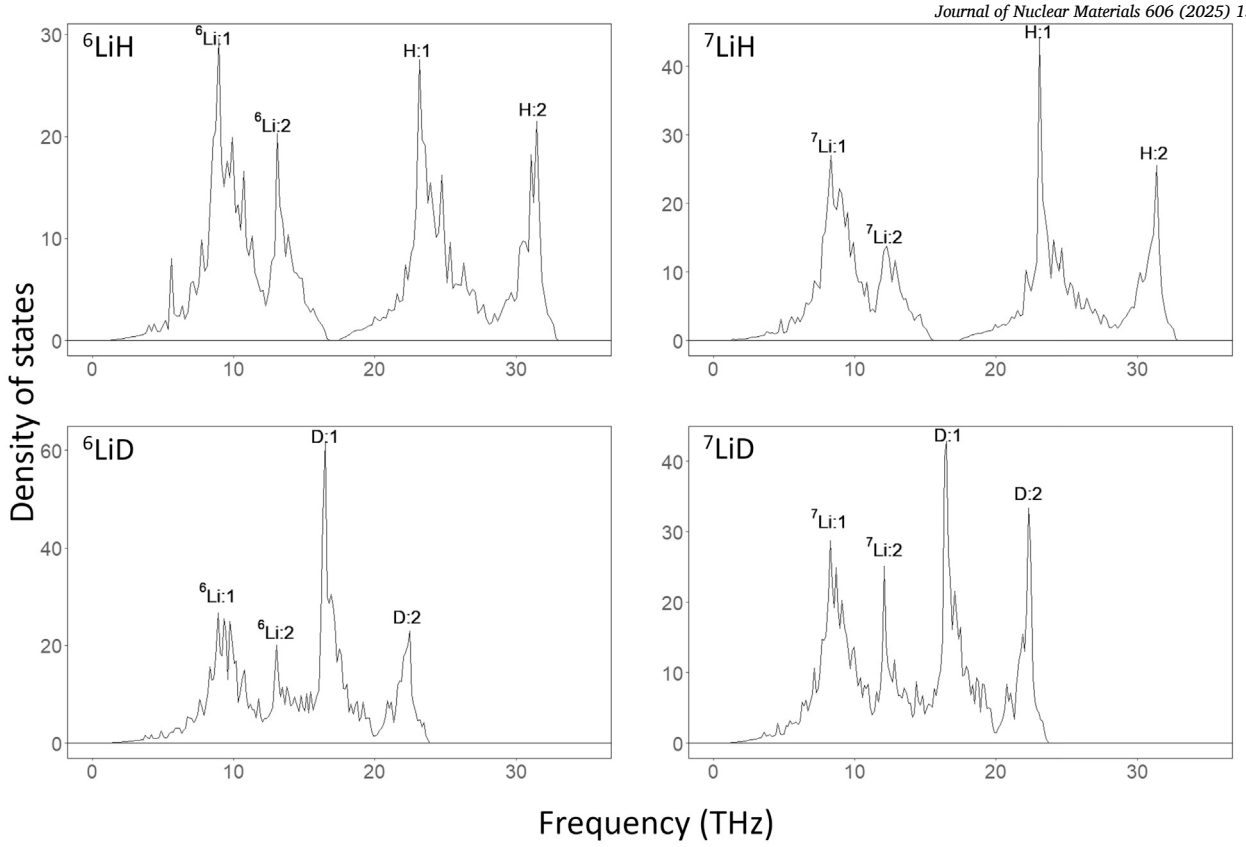

Fig. 3. Phonon density of states of lithium hydride isotopologues. The phonon density of states of lithium-6 hydride, lithium-7 hydride, lithium-6 deuteride and lithium-7 deuteride are arranged with their distinctive peaks labelled for each of the isotopes present in the target compounds.

[16–18] was applied after structural relaxation to extract the force constants and to calculate the phonon density of states (PDOS) [19]. These phonon calculated force constants were subsequently applied to determine the vibrational entropy of the lithium hydride isotopologues. The specific approach for the calculation of the force constants was through density functional perturbation theory (DFPT), which applies 3 displacements on each unique atom of the supercell, resulting in 189 different perturbations for the $2 \times 2 \times 2$ V_H supercell. In addition, this method was used to determine the zero point energy (ZPE) as determined by the background vibrations of a crystal system at 0 K. The entropy data for hydrogen gas (H_2) and deuterium gas (D_2) has been taken from the open-source thermochemical data tables compiled by NIST-JANAF, as used in previous DFT studies [20–22].

3. Results and discussion

3.1. Phonon density of states

Through the calculation of the phonon interactions of the isotopic lithium hydride systems, the phonon density of states (PDOS) were calculated, presenting the vibrational frequencies within the material in Fig. 3. No negative frequencies were observed, highlighting the stability of the systems as computed.

Significant differences are visible between the peaks associated with the two hydrogen isotopes, where the deuterium peaks (15-35 THz) are up-shifted, in comparison to the protium peaks (23-33THz). Whilst the ^{x}LiH and ^{x}LiD PDOS are different enough to differentiate the peaks to characterise the different hydrogen isotopes, there is a minimal difference between the peak positions between the lithium isotopes. The shifting of phonon peaks to lower frequencies with larger mass isotopes is the expected result and supports further analysis of the system and confidence in the subsequent results presented.

Table 1
Calculated enthalpy values of lithium hydride isotopologues. The vacancy formation enthalpies and the decomposition enthalpies of each of the lithium hydride isotopologues calculated during the initial computation are presented, whereby highlighting the similarities between the enthalpy values when modifying the lithium isotope.

Isotopologue	$\Delta H_{Single\ vacancy}$ (eV)	$\Delta H_{Decomposition}$ (eV)
^{6}LiH	1.15	0.73
^{7}LiH	1.15	0.73
^{6}LiD	1.21	0.76
^{7}LiD	1.21	0.76

3.2. Defect and reaction enthalpies

The internal energy of the isotopologues, as calculated by DFT, alongside the zero point energy (ZPE) as defined by the phonon interactions at 0 K (calculated through Phonopy) facilitates the calculation of the enthalpy of the four systems, including the vibrational correction, as shown by equations (3) and (4).

$$\Delta H_{Single\ vacancy} = (H_{V_H^{/}} + H_{\frac{1}{2}H_2} - H_{H_H^{\times}}) + (V_H^{/}\ ZPE - H_H^{\times}\ ZPE) \quad (3)$$

$$\Delta H_{Decomposition} = (H_{Li} + H_{\frac{1}{2}H_2} - H_{LiH}) + (Li\ ZPE - LiH\ ZPE) \quad (4)$$

For each of the isotopologues, Table 1 reports the change in enthalpy associated with the loss of one hydrogen from the supercell was calculated through equation (3), representative of a 3.125 at.% decrease in the total hydrogen concentration ($LiH_{0.97}$) and the loss of all hydrogen from the supercell, as described in equation (4).

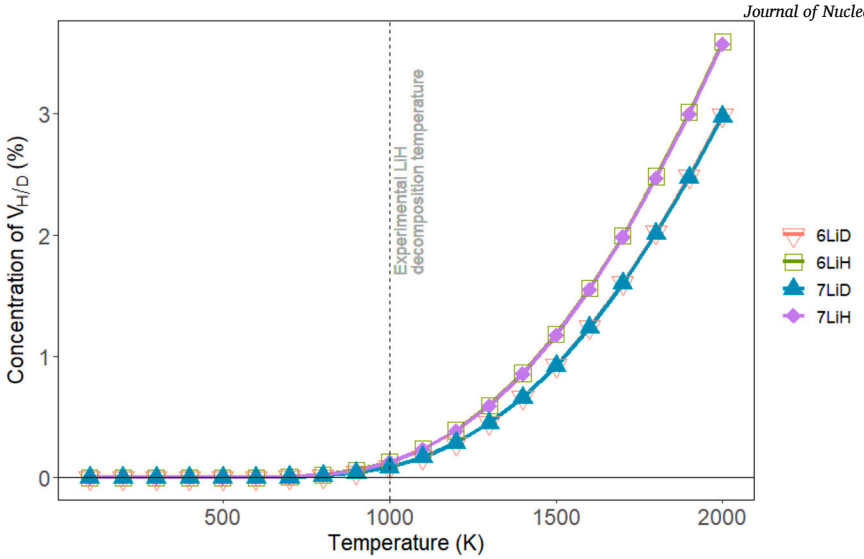

Fig. 4. Vacancy concentration of ^{x}LiH and ^{x}LiD. The predicted concentration of single hydrogen/deuterium vacancy in ^{6}LiH, ^{6}LiD, ^{7}LiH and ^{7}LiD using the enthalpy of defect formation (equation (3)) are shown across a range of temperatures, highlighting where the decomposition of lithium hydride occurs experimentally.

The difference between the hydrogen-containing and deuterium-containing isotopologues is due to the proportional weight change ($\Delta M_r = 2$) in the zero-point energy value (ZPE). There is a negligible difference between enthalpies, including the ZPE, of the lithium-6 and lithium-7 containing hydride/deuterides ($\Delta M_r = \frac{7}{6} = 1.17$).

Using the vacancy formation enthalpies of the lithium hydride isotopologues, the concentration of vacancies can be predicted using the law of mass action (equation (5)). Whilst the ZPE has an extremely small effect between the lithium isotopes resulting in inconsequential differences in the enthalpy computation (with the difference at the fourth significant figure), predicted differences when evaluating the defect concentrations at higher temperatures exist due to the enthalpy dependence of the calculation via this method.

$$[V_H] = exp(\frac{-\Delta H}{2KT}) \tag{5}$$

Fig. 4 shows that the hydride (containing ^{1}H) more readily releases its lattice hydrogen and becomes non-stoichiometric, with respect to lithium deuteride (containing ^{2}H). However, this is only significant above 1000 K where the concentration of the initial vacancies in the two LiX isotopologues visibly diverges, at which point the defect concentration is around 0.1% of the total crystal system. At 2000 K, well above the reported decomposition temperature, the predicted concentration of single hydrogen/deuterium vacancies is separated by 0.6 %, with lithium hydride's concentration being 3.6% compared to lithium deuteride's concentration being 3.0 %. The impact of vibrational entropy is now considered.

3.3. Free energy of decomposition

By considering the phonon contribution to the vibrational entropy, the change in free energy of the isotopologue systems is better calculated, comparing the vacancy formation and complete decomposition of the lithium hydride isotopologues.

$$\Delta G = \Delta H - T\Delta S \tag{6}$$

$$T = \frac{\Delta H}{\Delta S} \quad at\ \Delta G = 0 \tag{7}$$

The difference between the free energies associated with the initial isotopic hydrogen vacancy ($V_H^{/}$ and $V_D^{/}$) formation of each of the isotopologues from lithium hydride/deuteride (as described in equation (1)) was analysed, providing a temperature dependent hydrogen vacancy formation energy.

Fig. 5 identifies that at all temperatures the lithium hydride has a lower vacancy formation energy compared to the hydrogen vacancy formation energy in lithium deuteride. Additionally, loss of hydrogen isotopes becomes more facile with temperature when considering the vibrational entropy, becoming negative well-above the observed decomposition temperature of LiH, but significantly impacting the equilibrium vacancy concentration in both hydride and deuteride systems compared to the predictions where just enthalpy of formation is considered (Fig. 4).

Reapplying the law of mass action using the calculated free energies of each isotopologue for the initial vacancy formation allows for the determination of the effective defect concentration as affected by the vibrational entropy. The non-stoichiometry of ^{x}LiH at the experimental decomposition temperature 962 K is predicted to be approximately 12.1%, in agreement with the non-stoichiometry value reported in the experimental phase diagram (Fig. 1). Parallel to this, the non-stoichiometry of ^{x}LiD at the same temperature is predicted to be approximately 8.2% (Fig. 6).

At the experimental decomposition temperature of LiH, 962 K, the free energy values that take the vibrational entropy into consideration, the vacancy formation energy is lower by approximately 0.036 eV. As such, the predicted vacancy concentration when approaching the decomposition temperature is predicted to be larger when considering the free energy of the system, not just the formation enthalpy.

Alongside the consideration of initial isotopic hydrogen vacancy concentration, the difference between the free energies associated with the complete dehydriding/decomposition from the lithium hydride isotopologues to lithium metal and hydrogen gas (as described in equation (2)) was determined when including the vibrational entropy term, and the results presented in Fig. 7.

Fig. 7 confirms the presence of a clear pattern between the 4 isotopologues, with the lithium isotope playing a negligible role when considering the difference in dehydriding temperatures of each of the systems. The isotopologues containing hydrogen are observed to decompose at lower temperatures compared to their deuterium counterparts. Determining the temperatures which fulfil equation (7), LiH is reported to decompose at 959 K, in good agreement with the experimentally observed value of 962 K. Comparing these theoretical values against similar research on both the same material LiH [9] initially highlights that the decomposition temperatures which were determined are on the higher end of the whole spectrum, with the lowest recorded comparable temperature at 699 K whilst it was calculated as 959 K in this study,

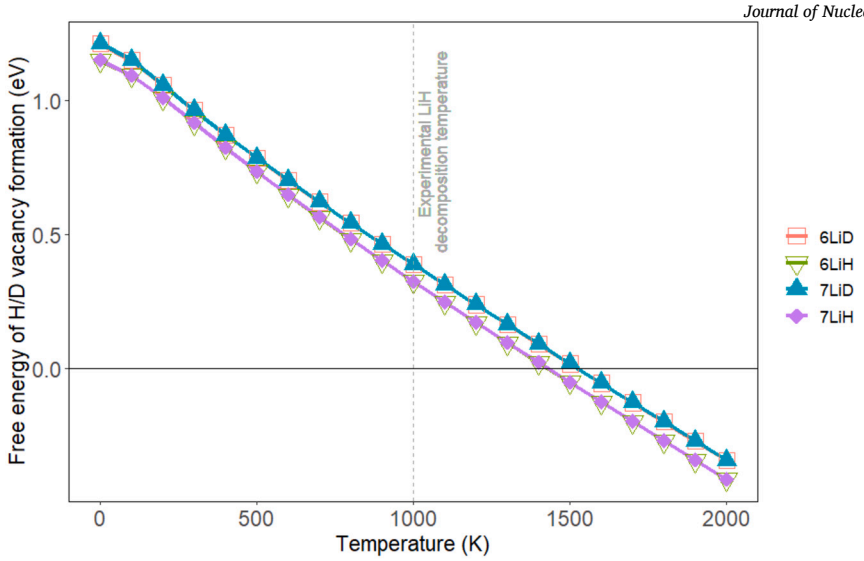

Fig. 5. Free energy of the initial vacancy formation for ^{x}LiH and ^{x}LiD. This plots the free energy of the decomposition as a function of temperature, showing the temperature dependence of the first isotopic dehydriding of lithium hydride isotopologues.

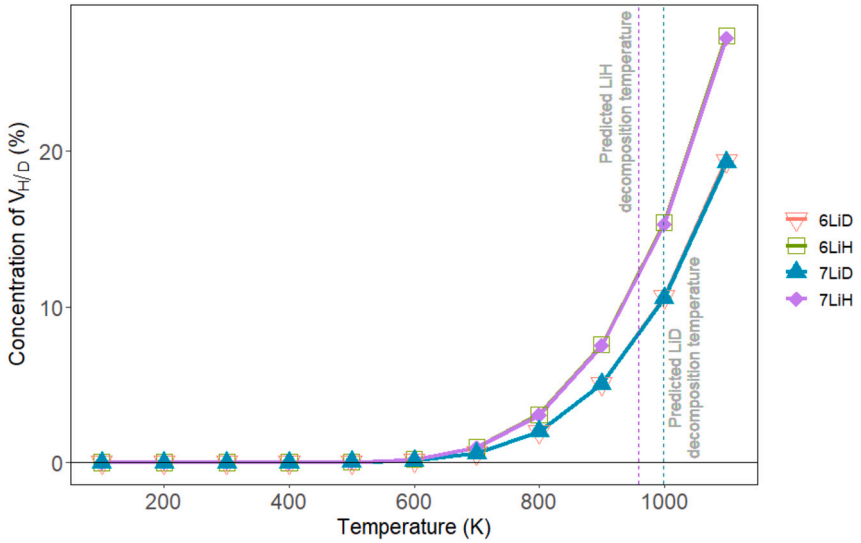

Fig. 6. The defect concentration [V_x] for ^{x}LiH and ^{x}LiD. This plots the calculated defect concentration [V_x] for each of the lithium hydride isotopologues when considering the free energy of vacancy formation as a function of temperature.

more aligning with practical analysis of hydrogen release and uptake [23] [24].

The LiD isotopologues are reported to decompose at 999 K, 40 K higher than LiH. This distinct behaviour between the isotopologues has relevance for the operation of the material within a fusion breeder system, with further work necessary to assess the behaviour of tritium and the deviations in stoichiometry, and combinations of hydrogen isotopes, that would result from its use within a fusion system. Comparing the difference between the affect of substituting hydrogen for deuterium within the compound against similar studies where the metal elements of the compound are replaced with transition metals, such as $MgXH_2$ [10], shows that this data follows a similar trend with the temperature of decomposition as a function of dopant concentration.

Finally, determining the concentration of vacancies for both the lithium hydride and deuteride using equation (5) at these decomposition temperatures results in $V_H = 11.8\%$ and $V_D = 10.6\%$ as displayed in Fig. 7, showing that at their respective decomposition temperatures the hydride is slightly more susceptible to the formation of non-stoichiometry than the deuteride as presented in Fig. 5, but they are broadly similar at their respective decomposition temperatures.

4. Conclusion

The importance of the incorporated hydrogen isotope has been highlighted as the key factor in the differentiation between the four lithium hydride isotopologues, creating distinct groupings in both the non-stoichiometry and decomposition behaviours. Contrasting this, the lithium isotope plays a negligible role in the discretisation of the isotopologues in comparison to the hydrogen/deuterium contribution. Furthermore, this work highlights that the hydrogen containing compounds require less energy to favour the dehydriding when compared to the deuterium containing compounds, and results in a proportionally larger concentration of defected material across a range of temperatures. Inversely, lithium deuteride requires a greater amount of energy (and therefore higher temperature) for it to decompose compared to the hydride, and possesses a smaller concentration of defects as temperature increases when vibrational entropy effects are considered. Defect concentration predictions are considerably altered when considering vibrational entropy in all systems considered.

The concentration of V_H at the computed decomposition temperature for ^{x}LiH (959 K) is reported as 11.8% and the concentration of V_D at

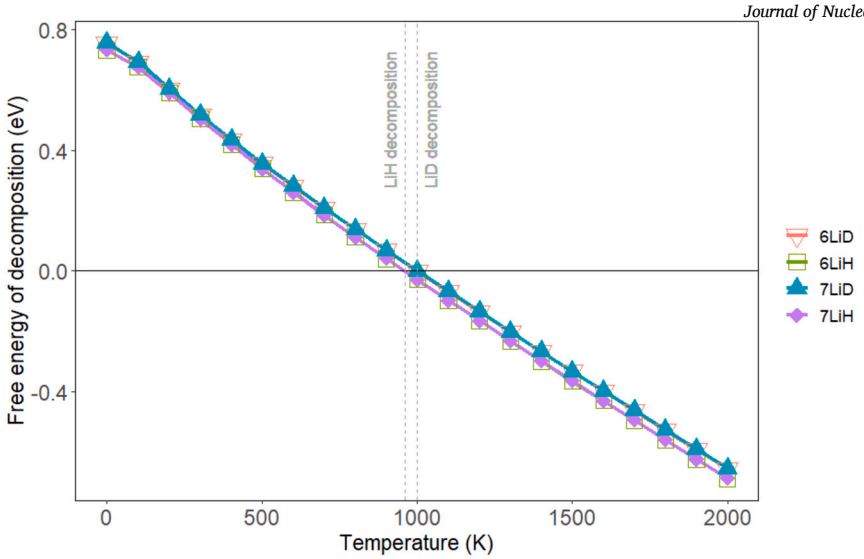

Fig. 7. Free energy of complete decomposition for ^{x}LiH and ^{x}LiD. This plots the free energy of the decomposition as a function of temperature, showing the temperature dependence of the complete isotopic dehydriding of lithium hydride isotopologues.

the computed decomposition temperature for ^{x}LiD (999 K) is reported as 10.6%. This highlights that, at the point of decomposition, the hydride containing isotopologues have similar degrees of non-stoichiometry at the point of decomposition; The difference in the decomposition temperature of lithium hydride and lithium deuteride is approximately 40 K independent of the lithium isotope. In comparison, in experimental literature, the temperature at which complete decomposition of LiH occurs is reported to be 962 K [2] highlights the acceptable predictive nature of the presented modelling work. Further work shall assess the impact of the isotopic abundance within mixed lithium hydride deuteride systems, including use of the Quasi-Harmonic approximation for phonon calculations.

The use of lithium hydride and lithium deuteride in breeder blanket concepts will need to incorporate the understanding of defect behaviour predicted in this work. As Li breeds the fusion fuel tritium, via neutron capture, the stocihiometry of the system will vary. Future work will consider the accommodation and transport of the tritium and helium products of ^{6}Li neutron fission reactions to identify the behaviour of the product in the LiH and LiD systems.

CRediT authorship contribution statement

Brandon J. Stratton: Writing – review & editing, Writing – original draft, Methodology, Investigation, Formal analysis, Data curation. **Thomas P. Davis:** Writing – review & editing, Supervision, Project administration. **Jack O. Astbury:** Writing – review & editing, Supervision, Funding acquisition, Formal analysis, Conceptualization. **Mohamad Abdallah:** Writing – review & editing, Funding acquisition. **Simon Stephens:** Writing – original draft, Visualization, Resources, Methodology, Data curation. **Simon C. Middleburgh:** Writing – review & editing, Writing – original draft, Supervision, Software, Resources, Project administration, Methodology, Investigation, Funding acquisition, Formal analysis, Data curation, Conceptualization.

Declaration of competing interest

The authors declare the following financial interests/personal relationships which may be considered as potential competing interests: Simon Middleburgh reports financial support was provided by Tokamak Energy Ltd. Brandon Stratton reports financial support was provided by Tokamak Energy Ltd. Simon Middleburgh reports a relationship with Tokamak Energy Ltd that includes: funding grants. Simon Middleburgh has patent #18267413 issued to Tokamak Energy. If there are other authors, they declare that they have no known competing financial interests or personal relationships that could have appeared to influence the work reported in this paper.

Acknowledgements

The research leading to these results was funded by Tokamak Energy Ltd. We are also grateful for the use of the Supercomputing Wales's resources which facilitated the majority of the calculations presented in this research. SCM was supported through Enhanced Methodologies for Advanced Nuclear System Safety (EP/T016329/1).

Data availability

Data will be made available on request.

References

[1] B.K. Rao, P. Jena, Molecular cluster calculations of the electronic structure of lithium hydride, J. Phys. C Solid State (1986), https://doi.org/10.1088/0022-3719/19/26/016.
[2] R.L. Smith, J.W. Miser, Compilation of the properties of lithium hydride, NASA Technical Memorandum, 1963.
[3] J. Graetz, J. Wegrzyn, J.J. Reilly, Regeneration of lithium aluminum hydride, J. Am. Chem. Soc. (2008), https://doi.org/10.1021/ja805353w.
[4] S. Banger, V. Nayak, U.P. Verma, Hydrogen storage in lithium hydride: a theoretical approach, J. Phys. Chem. Solids (2018), https://doi.org/10.1016/j.jpcs.2017.11.027.
[5] D. Simone, C. Bruno, Preliminary investigation on lithium hydride as fuel for solid-fueled scramjet engines, J. Propuls. Power (2009), https://doi.org/10.2514/1.39136.
[6] K.A. Yakimovich, T. Biryukova, Thermodynamic properties of li-lih (lid, lit) systems. The phase diagram, Open J. Phys. Chem. (2012), https://doi.org/10.4236/ojpc.2012.23019.
[7] R. Liu, Y. Peng, W. Rong, Q. Cao, Thermodynamics and kinetics hydrogen isotope effects of hydrogen/deuterium absorption in pd-5wt.%pt alloy, Int. J. Hydrog. Energy (2023), https://doi.org/10.1016/j.ijhydene.2023.07.329.
[8] P.A.T. Olsson, A.R. Massih, J. Blomqvist, A.M. Alvarez Holston, C. Bjerkén, Ab initio thermodynamics of zirconium hydrides and deuterides, Comput. Mater. Sci. (2014), https://doi.org/10.1016/j.commatsci.2014.01.043.
[9] S. Bahou, H. Labrim, M. Lakhal, H. Ez-Zahraouy, Improving the hydrogen storage properties of lithium hydride (lih) by lithium vacancy defects ab initio calculations, Solid State Commun. (2023), https://doi.org/10.1016/j.ssc.2023.115167.
[10] S. Bahou, H. Labrim, H. Ez-Zahraouy, Role of vacancies and transition metals on the thermodynamic properties of mgh2: ab-initio study, Int. J. Hydrog. Energy (2023).
[11] J. Furthermüller, G. Kresse, Efficient iterative schemes for ab initio total-energy calculations using a plane-wave basis set, Phys. Rev. B, Condens. Matter (1996), https://doi.org/10.1103/PhysRevB.54.11169.

[12] J.P. Perdew, K. Burke, M. Ernzerhof, Generalized gradient approximation made simple, Phys. Rev. Lett. (1996), https://doi.org/10.1103/PhysRevLett.77.3865.

[13] B. Hammer, L.B. Hansen, J.K. Norskov, Improved adsorption energetics within density-functional theory using revised Perdew–Burke–Ernzerhof functionals, Phys. Rev. B (1999), https://doi.org/10.1103/PhysRevB.59.7413.

[14] F.A. Kröger, H.J. Vink, Relations between the concentrations of imperfections in crystalline solids, Solid State Phys. (1956), https://doi.org/10.1016/S0081-1947(08)60135-6.

[15] E.G. Seebauer, M.C. Kratzer, Charged Semiconductor Defects, Springer, 2008.

[16] A. Togo, I. Tanaka, First principles phonon calculations in materials science, Scr. Mater. (2015), https://doi.org/10.1016/j.scriptamat.2015.07.021.

[17] A. Togo, First-principles phonon calculations with phonopy and phono3py, J. Phys. Soc. Jpn. (2023), https://doi.org/10.7566/JPSJ.92.012001.

[18] A. Togo, L. Chaput, T. Tadano, I. Tanaka, Implementation strategies in phonopy and phono3py, J. Phys. Condens. Matter (2023), https://doi.org/10.1088/1361-648X/acd831.

[19] G. Roma, C.M. Bertoni, S. Baroni, The phonon spectra of lih and lid from density-functional perturbation theory, in: Solid State Commun., 1996.

[20] Malcolm W. Chase Jr., Nist-janaf thermochemical tables, J. Phys. Chem. Ref. Data (1998), https://doi.org/10.18434/T42S31.

[21] C.M. Moore, J. Wilson, M.J.D. Rushton, W.E. Lee, J.O. Astbury, S.C. Middleburgh, Hydrogen accommodation in the tizrnbhfta high entropy alloy, Acta Mater. (2022), https://doi.org/10.1016/j.actamat.2022.117832.

[22] S.C. Middleburgh, A. Claisse, D.A. Andersson, R.W. Grimes, P. Olsson, S. Mašková, Solution of hydrogen in accident tolerant fuel candidate material: U3si2, J. Nucl. Mater. (2018), https://doi.org/10.1016/j.jnucmat.2018.01.018.

[23] L. Wang, M.Z. Quadir, K.F. Aguey-Zinsou, Direct and reversible hydrogen storage of lithium hydride (lih) nanoconfined in high surface area graphite, Int. J. Hydrog. Energy (2016), https://doi.org/10.1016/j.ijhydene.2016.07.073.

[24] L. Wang, M.Z. Quadir, K.F. Aguey-Zinsou, Ni coated lih nanoparticles for reversible hydrogen storage, Int. J. Hydrog. Energy (2016), https://doi.org/10.1016/j.ijhydene.2016.01.173.